Tellus (1998), 50B, 449–462
Printed in UK – all rights reserved

TELLUS
ISSN 0280–6509

Analysis of the growth of nucleation mode particles observed in Boreal forest

By MARKKU KULMALA, ANNE TOIVONEN, JYRKI M. MÄKELÄ and ARI LAAKSONEN*[1],
Department of Physics, POB 9, 00014 University of Helsinki, Finland; [1]*University of Kuopio, Department of Applied Physics, POB 1627, 70211 Kuopio, Finland*

(Manuscript received 21 July 1997; in final form 27 August 1998)

ABSTRACT

Aerosol formation and subsequent particle growth in the ambient air have been frequently observed at a boreal forest site, Southern Finland. During a 1-year period we have observed significant aerosol formation on more than 50 days. Submicron aerosol size distributions have been measured using differential mobility analyzing technique. On several days, the growth of nucleation mode particles to Aitken mode has been observed to take place within $\sim$10 h subsequent to their formation at a rate of a few nm/h. 10 days of the data, representing the particle formation days with a clear subsequent growth, were selected for a closer examination. The growth of nucleation mode particles was analysed with an integral aerosol dynamics model. The model includes photochemical formation of a condensable compound in the gas phase, condensation and particle coagulation. The observed particle growth of the nucleation mode particles can be explained by continuum/transition regime condensation theory. The model gives the gas-phase concentration of the condensing species as a function of time. Since the actual condensing species has not been experimentally identified, the molecular properties of the condensing compound were varied in the model. This sensitivity study revealed that the molecular properties have only a small effect on the daily maximum concentration of the condensing species. We also studied the sensitivity of the results to variations in the source term of the condensable species and to variations in temperature and relative humidity. Accounting for the results of the sensitivity studies, we conclude that the maximum daily concentration of gas-phase, condensing molecules achieved at the site was greater than 10^7 cm^{-3}, while their saturation vapor density is below 10^5 cm^{-3}.

1. Introduction

The study of atmospheric aerosol formation has recently received growing interest (see e.g. Weber et al., 1995; Wiedensohler et al., 1996). One reason for this interest is that aerosol particles affect the radiation balance of the Earth both directly and indirectly (Charlson and Wigley, 1994). The formation and growth of aerosol particles are strongly influenced by condensation processes. The nucleation and condensational growth of aerosols require the presence of low vapour-pressure molecular species in the gas phase. The source term of such species may be direct emissions or chemical reactions, whereas condensational depletion is their most important sink term.

Condensational growth of aerosol particles has been studied in detail both theoretically and experimentally (Vesala et al., 1997, and references therein). These studies have shown clearly that the coupling between the mass fluxes of different condensing vapours and the heat flux is strong. Rudolf et al. (1991), Rudolf (1994) performed laboratory experiments demonstrating that binary

* Corresponding author.
e-mail: ari.laaksonen@uku.fi

vapour mixtures significantly boost condensational growth. In their studies, nitric acid as well as alcohols were used together with water vapour. The mass flux of water vapour was increased by as much as several orders of magnitude when, e.g., nitric acid participated in the condensational growth process.

It has also been theoretically shown that multicomponent droplets can grow easier than one component or binary droplets. Mattila et al. (1997) simulated mixtures of different alcohols and water, as well as various water–acid–ammonia systems. According to their results, even small amounts of condensing gases other than water affect the growth curves significantly.

McMurry and Wilson (1982) discussed different aerosol growth mechanisms and the growth laws to which different mechanisms lead. They introduced a numerical method, applied also by Juozaitis et al. (1996), to obtain a growth law from the size distribution measurement data. However, in the atmosphere, condensational growth of freshly formed aerosol particles is usually slow at relative humidities below 90–95%. This is because the concentrations of condensable species other than water are low in absolute terms, and thus the condensational growth of particles takes a long time (from hours to days). The long timescales, combined with naturally occuring fluctuations in aerosol particle concentrations and size distributions, make it rather difficult to apply the McMurry-Wilson technique to atmospheric aerosol data, and produce often rather large error margins to the calculated growth rates (Toivonen, 1997).

Kerminen and Wexler (1996) performed a theoretical study applying different growth laws to explain the split of the accumulation mode into two individual modes, formerly known as Aitken and accumulation mode. However, these growth laws include cloud processings, chemical reactions etc.

Weber et al. (1997) estimated ambient nanoparticle growth rates from their measurements by two independent methods. Firstly, they measured sulphuric acid vapour concentrations and particle concentrations in the size range of 2.7–4 nm, and derived the growth rate from the time lag between these two, i.e. the disappearance of acid vapour versus rise and fall of nanoparticle number concentration. Secondly, they also estimated growth laws from linking together nanoparticle concentration vs. particle surface area obtaining the amount of cluster scavenging on the surface.

We have recently shown (Mäkelä et al., 1997) that new particles are frequently formed at a boreal forest site in southern Finland. This paper focuses on the growth of the submicron particles subsequent to the actual nucleation event. Ten days of the 1996 data were chosen under a closer examination. We will present experimental evidence of nucleation mode particles growing to Aitken mode within 10 hours. Using an aerosol dynamics model, we will also show that the observed growth can be explained by a condensation mechanism (below, we will use the term "condensational growth" and "condensation" to indicate gas-phase kinetics and/or diffusion limited growth with no chemical reactions occurring on the surfaces or in the volume of the aerosol particles). The main result of our model calculations is an estimate of the density of the condensing vapour.

2. Experimental

The boreal forest measurement station "SMEAR II" in Hyytiälä (Station for Measuring forest Ecosystem–Atmosphere Relations, central southern Finland, 61 51′ N, 24 17′ E) was built to provide a cross disciplinary co-operation between atmospheric, silvicultural, soil and forest ecological studies on fluxes of different compounds in Scots pine forest (Pinus sylvestris). The terrain of the measurement site is relatively flat and located within a forest of 30 years of age. Understorey species consist of Calluna vulgaris, Vaccinium myrtillus and various mosses. The nearest urban sources are the cities of Tampere ($\sim$50 km SW) and Jyväskylä ($\sim$100 km NE). The station has facilities to measure CO_2, H_2O, SO_2, O_3, and NO_x concentrations as well as the exhange of these gases between plants, temperature, wind speed and direction, irradiation (photoactive, global, reflected, net, diffusive, UVA, UVB), rain and air pressure. The general goal of the station is to understand the behaviour of air pollutants in the atmosphere and their consequences in the environment, combining physico-chemical and biological expertise (SMEAR-homepage, 1997).

The sample flow for measuring the aerosol

number size distribution is presently taken through the eastern wall of a 60 m^2 cottage at the height of 2 m from the ground. The primary flow is $\sim$25 m^3/h from where the particle sample flow (2.5 l/min) is drawn to the actual instrumentation. Charge equilibrium for the particles in the sample flow is obtained by use of a bipolar ^{85}Kr aerosol neutralizer (TSI Model 3077). For measuring the particle number size distribution we use conventional electrical mobility analysis of submicron particles (Knutson and Whitby, 1975), where narrow electrical mobility increments are extracted in turn from the ambient size distribution and transferred into the condensation particle counter. In our set up we use two differential mobility analyzer (DMA) systems covering two subranges in particle size, slightly overlapping with each other. The sample flow is split into two Vienna type DMA's (11 and 28 cm; see Winklmayr et al., 1991), which are used for electromobility size classification of the particles running with sheath air volume flow rates of 10 and 22 l/min. For monodispersed particle detection after each classification, two condensation particle counters are used: TSI Model 3010 (Agarwal and Sem, 1980; Mertes et al., 1995) and TSI Model 3025 (Stolzenburg and McMurry, 1991; Kesten et al., 1991). The voltages on the DMA cylinders are maintained using two high voltage supplies (FUG 1250 V and FUG 12500 V). The sheath flows of the DMAs are maintained utilising a closed sheath air loop using critical orifices (Jokinen and Mäkelä, 1997). The sheath flows are not treated by additional dryers etc., and thus the particle size is measured close to ambient conditions. With this instrumentation the size ranges of 3–25 nm and 20–500 nm (particle diameter) are covered. When the two spectra are finally combined, the number size distribution in the range of 3–500 nm is obtained (for standard electromobility analysis, see e.g. Kousaka et al., 1985 or Reischl, 1991). The actual measurement cycle for the whole size range is 10 minutes.

3. Theoretical

3.1. Model

The growth of nucleation mode particles was analysed with a three mode (representing nucleation, Aitken and accumulation modes) integral aerosol dynamics model (Kulmala et al., 1995; Pirjola and Kulmala, 1998). The model includes oxidation of a precursor P in the gas-phase to form a water-soluble, condensable product X, condensation of vapours on pre-existing particles, and coagulation. The time evolution of the size distribution of aerosol is followed by integrating the differential equations of the particle number concentration, particle mass concentration and condensing vapour concentration (sulphuric acid as an example). The simple model used in the present study is accurate enough to estimate the concentration of the condensable vapour.

Consider the condensable molecule X. The time dependence of the vapour concentration of X (N_X) can be presented by

$$\frac{dN_X}{dt} = Q_X - C_1(N_X, N_1, Y_0(\mathrm{Ke})) - C_2(N_X, N_2, Y_0(\mathrm{Ke})) - C_3(N_X, N_3, Y_0(\mathrm{Ke})), \quad (1)$$

where N_i is the total number concentration of particles in mode i, Q_X is the source term of gaseous X determined by the gas phase oxidation rate of P, and C_i is the condensation rate of X-molecules on particles with mass $m_{\mathrm{par},i}$. Index 1 refers to nucleation mode particles, 2 refers to Aitken mode particles and 3 to accumulation mode particles. C_i is a function of vapour concentration of X, the total number concentration of particles in a mode, and saturation vapour density (Y_0) times the Kelvin effect (Ke). The aerosol size distribution is described by the mean masses of particles in modes $i = 1 \ldots 3$ ($m_{\mathrm{par},i} = M_i/N_i$) and the corresponding radii. M_i denotes the total particle mass in every mode.

The time evolution of the particle number concentrations due to coagulation is given by

$$\frac{dN_1}{dt} = -0.5K_{11}N_1N_1 - K_{12}N_1N_2 - K_{13}N_1N_3, \quad (2)$$

$$\frac{dN_2}{dt} = -0.5K_{22}N_2N_2 - K_{23}N_2N_3, \quad (3)$$

$$\frac{dN_3}{dt} = -0.5K_{33}N_3N_3, \quad (4)$$

where K_{ij} is the coagulation coefficient between a particle in mode i and a particle in mode j. The coagulation coefficients are calculated assuming

that K_{ij} is the brownian coagulation coefficient between particles of radii r_i and r_j corresponding to masses $m_{\mathrm{par},i}$ and $m_{\mathrm{par},j}$.

The time evolution of particle mass concentrations in the three modes is given by

$$\frac{\mathrm{d}M_1}{\mathrm{d}t} = C_1 m_{\mathrm{X}} + C_1 m_{\mathrm{w}} \frac{(1-x_1)}{x_1} \times \left(N_{\mathrm{X}} - Y_0 \exp\left(\frac{2\sigma m_{\mathrm{X}}}{kT\rho R_1}\right)\right) N_1 - K_{12} N_1 N_2 m_{\mathrm{par},1} - K_{13} N_1 N_3 m_{\mathrm{par},1}, \quad (5)$$

$$\frac{\mathrm{d}M_2}{\mathrm{d}t} = C_2 m_{\mathrm{X}} + C_2 m_{\mathrm{w}} \frac{(1-x_2)}{x_2} \times \left(N_{\mathrm{X}} - Y_0 \exp\left(\frac{2\sigma m_{\mathrm{X}}}{kT\rho R_2}\right)\right) N_2 + K_{12} N_1 N_2 m_{\mathrm{par},1} - K_{23} N_2 N_3 m_{\mathrm{par},2}, \quad (6)$$

$$\frac{\mathrm{d}M_3}{\mathrm{d}t} = C_3 m_{\mathrm{X}} + C_3 m_{\mathrm{w}} \frac{(1-x_3)}{x_3} \times \left(N_{\mathrm{X}} - Y_0 \exp\left(\frac{2\sigma m_{\mathrm{X}}}{kT\rho R_3}\right)\right) N_3 + K_{13} N_1 N_3 m_{\mathrm{par},1} + K_{23} N_2 N_3 m_{\mathrm{par},2}. \quad (7)$$

Here, x_i is the mole fraction of molecule X in the particles, m_{X} and m_{w} are the molecular masses of X and water, respectively, σ is surface tension, and $R_1 \ldots R_3$ are the mean radii of the three modes. The partial vapour density of condensing molecules over the surface of the solution droplet is estimated by saturation vapour density times the Kelvin effect.

Oxidation of the gas-phase precursor is described by:

$$\text{precursor} + \text{radical} \rightarrow \text{product}. \quad (8)$$

The chemical composition of the observed nucleation mode particles is unknown. In principle we have several candidates for precursors, e.g. terpenes and SO_2. In this study, we assume that the precursor P reacts with the OH-radical to form species X. In this case the expression for the source term is

$$Q_{\mathrm{X}} = k_{\mathrm{X}}[\mathrm{OH}][\mathrm{P}]. \quad (9)$$

The rate determining reaction for the formation of X is the reaction of P with the OH-radical. The temperature and pressure dependences of the rate constant k_{X} are taken to be the same as those given by DeMore et al. (1985) for $k_{\mathrm{H_2SO_4}}$. We stress that, although the sulphuric acid rate constant is used, the P-X-system applied in our calculations should be considered a model system only; our aim is to study features of the observed growth that are more or less independent of the molecular nature of the condensing species.

3.2. *Condensation of model molecules*

The condensation mechanism was assumed to be either binary condensation of X and H_2O or one-component condensation of X alone. In order for the water molecules to enhance the condensation rate as much as possible compared with the one-component case, the values of the activity coefficients of the liquid X/H_2O solution have to be as low as possible. They were therefore modeled after the sulphuric acid/water solution (Jaecker-Voirol 1988). An approximate method was applied to calculate the binary condensation rate (Kulmala, 1990). We assumed that the vapour concentration of X is low compared with that of H_2O, and therefore a new solution droplet reaches equilibrium with water vapour quickly. The growth rate of the droplets depends on the absorption of the X molecules into the droplets. Once absorption has taken place, the composition of the droplets changes. An increase in the weight percentage of X in the droplets causes the partial vapour pressure of water above the solution surface to become lower than before absorption. The droplet is unsaturated with respect to water vapour, and more water vapour molecules can be absorbed by the droplet until a new equilibrium condition is reached.

The condensation rate of X molecules, (C_{X}), into a liquid droplet of radius R is:

$$C_{\mathrm{X}} = N_{\mathrm{p}} \frac{\mathrm{d}n_{\mathrm{X}}}{\mathrm{d}t}, \quad (10)$$

where N_{p} is number density of the (monodisperse) particles. The continuum/transition regime condensation theory is adopted. Thus

$$\frac{\mathrm{d}n_{\mathrm{X}}}{\mathrm{d}t} = 4\pi R \beta_{\mathrm{M}} D \left(N_{\mathrm{X}} - Y_0 \exp\left(\frac{2\sigma m_{\mathrm{X}}}{kT\sigma R}\right)\right), \quad (11)$$

where N_{X} is vapour concentration, and R refers to the mean radius of nucleation, Aitken or accumulation mode. The transitional correction factor,

β_M, is (Fuchs and Sutugin, 1970)

$$\beta_M = \frac{K_n + 1}{0.377K_n + 1 + \frac{4}{3}\alpha^{-1}K_n^2 + \frac{4}{3}\alpha^{-1}K_n}, \quad (12)$$

In eq. (12) α is the the sticking coefficient, and the Knudsen number is

$$K_n = \frac{\lambda_v}{R}. \quad (13)$$

The mean free path of vapour molecules, (λ_v), is connected to the diffusion coefficient, (D), through

$$\lambda_v = 3\sqrt{\frac{\pi m_X}{8kT}}D. \quad (14)$$

The diffusion coefficient can be expressed as a function of diffusion volumes of air, d_{air}, and the condensing vapour, d_X,

$$D = \frac{10^{-3}T^{1.75}\sqrt{\frac{1}{m_{air}} + \frac{1}{m_X}}}{p(d_{air}^{1/3} + d_X^{1/3})^2}, \quad (15)$$

where m_{air} and m_X denote the molecular masses of air and the condensing substance, and p is pressure in atm (Reid et al., 1987).

4. Results

4.1. Observations

Number size distributions of atmospheric submicron aerosols have been measured on a continuous basis since 31 January 1996. During the first one-year period we have observed significant aerosol formation and subsequent growth on more than 50 days (Mäkelä et al., 1997). The Aitken and accumulation modes are always present, but on the majority of the days nucleation mode is present only temporarily. Clear growth of nucleation mode particles occurs only on the particle formation event days, mentioned above. Figs. 1 and 2 show typical daily variations of temperature profile, relative humidity profile and global radiation during a nucleation event day. The temperature and relative humidity have been measured at 6 different heights. During night time the air is cooler at ground level than at higher levels. Several hours after sunrise (around 8 o'clock) the temperature profile changes its direction (Fig. 1a) causing vertical mixing. Although the relative humidity profile is not as clear as the temperature profile, a clear daytime minimum can be seen (Fig. 1b). The midday R.H. peak is not usual and we do not have an explanation for it. It appears to be associated with changes in the slopes of the temperature and radiation curves (Fig. 2), and could be due to evaporation or mixing.

The daily variation of global radiation on a sunny day exhibits the form of a sine curve (Fig. 2), but if the mixing is accompanied by cloud forma-

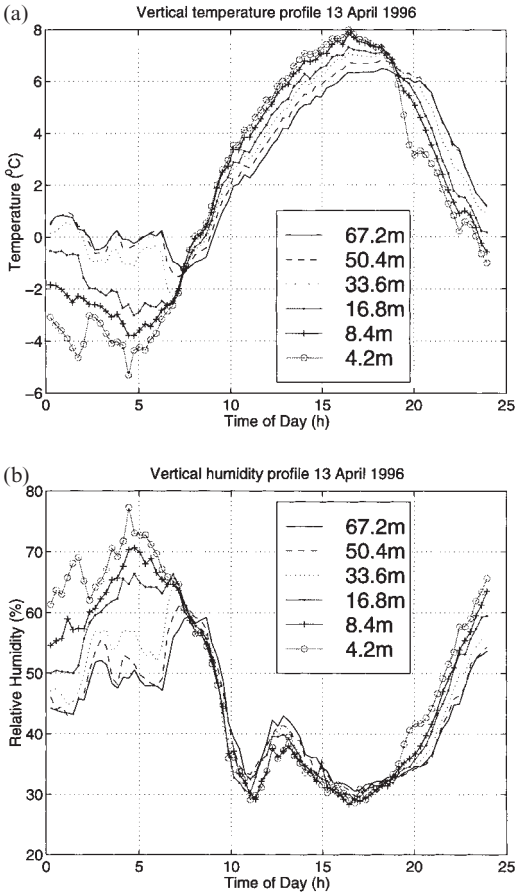

Fig. 1. Measurement data at different levels from the 73 m high tower at the Hyytiälä measurement site, on 13 April. (a) Temperature data. The clear "flip-over" in the vertical temperature profile at 7–8 a.m., is often observed to occur in connection with the particle formation events. (b) Relative humidity data. The RH data have been deducted from measurements on temperature and water vapour concentration at different levels, on 13 April.

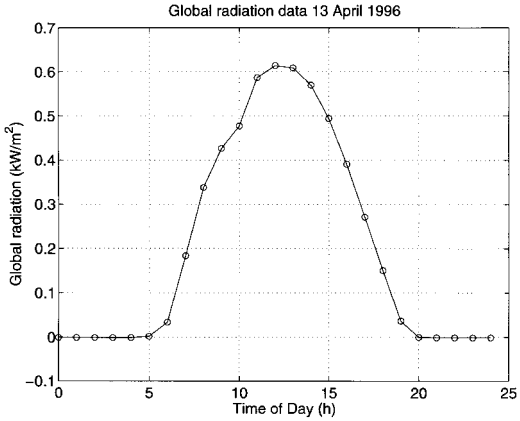

Fig. 2. Hourly averages of the global radiation measured above canopy (15 m above ground) in Hyytiälä on 13 April with Pyranometer Reemann TP-3 ($\lambda =$ 0.3–4.8 μm). The days with nanoparticle formation and growth tend to have a sunny morning (before vertical mixing takes place).

tion, the global radiation curve contains a clear deviation from the sinusoidal shape during the morning hours. The appearance of new ultrafine particles occurs on the average 4 h after the sunrise. On April 13 (Figs. 1, 2) the first ultrafine particles were detected at 8:30 a.m., i.e. 3.5 h after sunrise. Systematically, the particle formation events start not earlier than 2 h after sunrise. It is known that the particle formation and subsequent growth requires sunlight. To interpret our data, we have at least two qualitative explanations. Either the sunlight of the morning hours drives photochemistry producing condensable vapour or, alternatively, the vertical mixing generates suitable thermodynamical conditions for the nucleation/condensation to occur. Mixing could also carry some additional chemical species from the free troposphere that take part in the mass transfer from gas to particulate phase. Besides, the particles could be generated aloft and mixed down. However, although radiation is necessary for a nucleation event to occur, the actual absolute amount of sunlight, during the event or integrated from sunrise to the beginning of the event, cannot be directly correlated with number concentration of new particles or the extent of their growth. Furthermore, during, e.g., hot and sunny summer days, particle formation events rarely occur.

The experimental data of particle distributions during 10 nucleation event days are presented in Figs. 3, 4. The existence of Aitken mode can be seen in all 10 figures, and in some cases also a clear accumulation mode is seen. The data shows that the nucleation mode appears typically before noon (in spring, summer and early autumn) or some hours after noon (October). The time of nucleation mode formation is connected with global radiation. The earlier the sun rises the earlier the nucleation mode appears, the average delay time being 4 h. From the data one can also see that the growth from nucleation mode to Aitken mode takes typically less than 10 hours. In June the growth was significantly faster than during the other days. The particles grew to 60–70 nm in June and to 30–40 nm in the spring and autumn.

Our data on total particle concentrations show often a decrease before the nucleation mode appears. This would indicate that the vertical mixing of air parcels typically occurs before or during particle formation. To analyze the concentration decrease in more detail, we calculated the Aitken and accumulation mode concentrations (using a non-linear least squares fitting method) an hour before and an hour after the beginning of a nucleation event for all of the 55 events observed in 1996. The accumulation mode concentrations did not show a decrease more often than an increase. However, the Aitken mode concentrations decreased in 67% of the events studied. Fig. 5 is a frequency plot of the ratio of Aitken mode concentrations after and before the event. The median of $N(\text{after})/N(\text{before})$ is 0.83. It thus seems that the beginning of a nucleation event is often associated with mixing of air cleaner with respect to Aitken mode aerosol particles.

The growth curves (or bands) seen in Figs. 3, 4 are continuous, and this is the case with most of the over 120 nucleation events we have recorded so far. Only in very few cases does the nucleation mode suddenly disappear after a growth of a few hours. This clearly suggests that the nucleation events occur over a large area; if the area was limited, the air would have to be very still (which is often not the case as shown by our wind speed data) in order for the growing particles not to disappear because of mixing. Furthermore, we have evidence from simultaneous measurements in Hyytiälä and in the Helsinki area that the

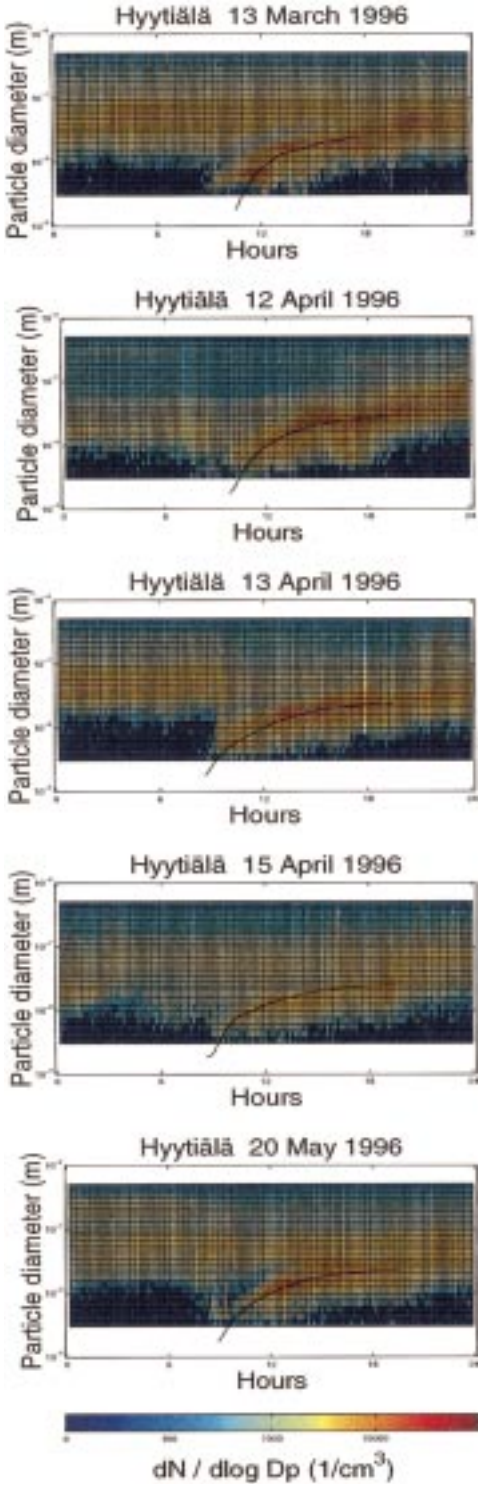

Fig. 3. Daily size distribution data (10-min intervals) of five particle formation days in Hyytiälä chosen for closer examination in this paper. Particle formation can be seen as a red band arising from 3 nm before midday and the growth occurs towards 30–40 nm later on the afternoon. The black lines are modeled growth curves.

nucleation events can occur over areas hundreds of kilometers wide.

4.2. Model calculations

Encouraged by the indication that we are sampling the same airmass all of the time when a continuous growth curve is recorded, we decided to apply our aerosol model in a non-Lagrangian way, i.e., as though the aerosol we are measuring would have been formed and growing at the measurement location. This is a similar approach to those of McMurry and Wilson (1982), Juotzaitis et al. (1996), and Weber et al. (1997): Although their techniques of analysing the measured aerosol distributions were different from ours, they relied on the assumption that measurements performed for several hours at a single location would reveal the aerosol growth mechanism. We are well aware that the assumption of nucleation mode size evolution occuring close to where we are measuring may not be valid: The nucleation might for example have taken place in the upper layers of the boundary layer, and the aerosol we sample in the evening might have spent most of the day at a different temperature and relative humidity than that measured at our station. We therefore performed a sensitivity analysis, described below, in which temperature and relative humidity were varied from those recorded at the location. The sensitivity analysis did not change our main result, an order-of-magnitude estimate of the gas-phase concentration of the condensing molecular species.

The aerosol dynamics model described above was used in order to find out whether the observed particle growth is condensational (i.e., limited by kinetics and/or diffusion depending on particle size, rather than by surface or volume reactions). 10 days (shown in Figs. 3, 4), during which the growth of nucleation mode particles was clearly seen, were selected to be analysed. The selected days represented seasons from early spring to late autumn. The initial values of particle number densities and sizes in each of the three modes

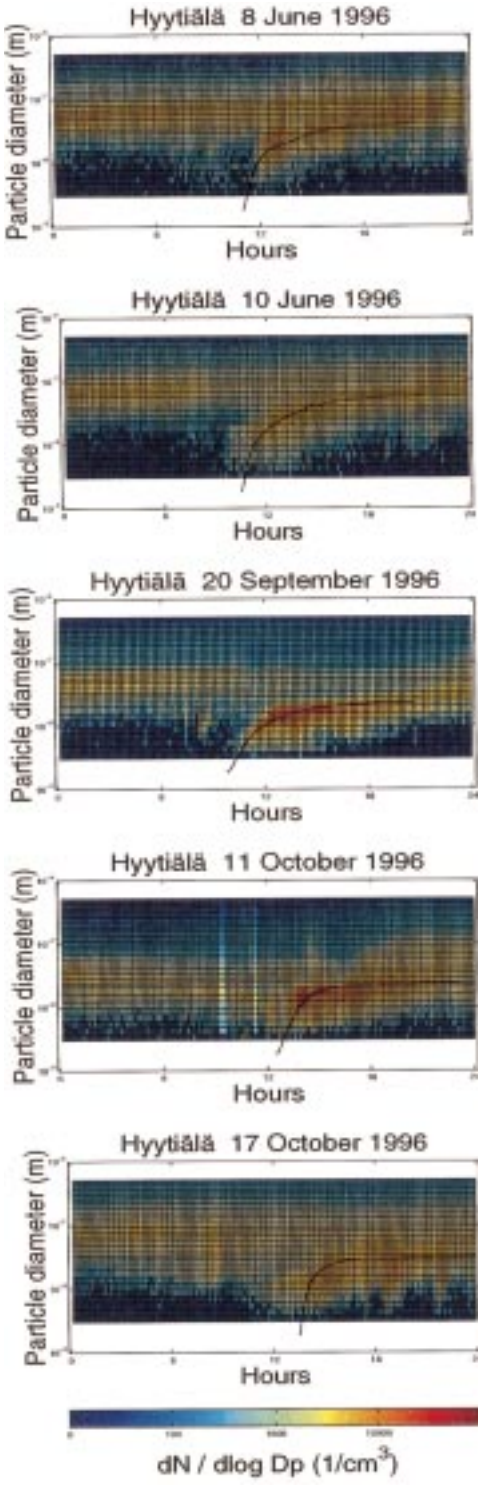

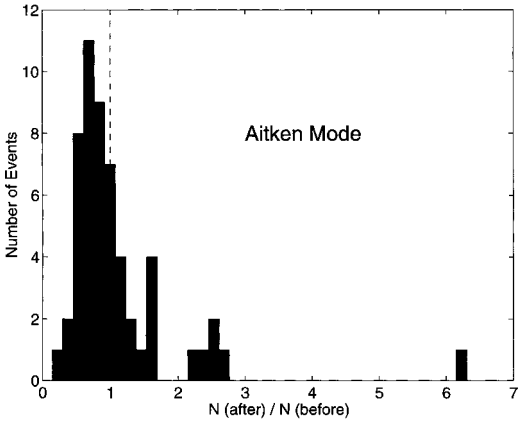

Fig. 5. Frequency plot of the ratio of Aitken mode concentration an hour after the beginning of a nucleation event to Aitken mode concentration an hour before the beginning of the event.

needed in the model calculations were taken from the measurement data. Temperature, relative humidity and global radiation are recorded continuously at the location, and their values were updated in the model every 18 minutes (global radiation every hour). The source term of the condensable vapour molecules was divided into two parts. One part of the source term was kept constant and the other part was set to depend linearly on global radiation.

As explained above, we assumed that the condensing molecule X is formed in the reaction of the precursor P with the hydroxyl radical. Thus the constant part of the source term is taken to be [P] (which is assumed to have a considerably higher gas-phase concentration than the condensable product X) and the variable term is [OH]. The measured values of global radiation (W/m^2) were numerically multiplied by 10^7 to produce the approximate level of [OH] ($molecules/cm^3$). The concentration of species P, on the other hand, was adjusted in order to reproduce the observed growth of the nucleation mode particles as accurately as possible. After finding a suitable level, the

Fig. 4. Daily size distribution data (10-min intervals) of 5 particle formation days in Hyytiälä chosen for closer examination in this paper. Here the nucleation mode grows towards 60–70 nm in June and towards 30–40 nm in the autumn. The black lines are modeled growth curves.

concentration of P was kept constant during one simulation.

The particle number concentrations and the mean radii in the Aitken mode and in the accumulation mode were taken from the size distribution data. These two modes were fitted to the size distribution data by a non-linear least squares method. The initial mean diameter of the nucleation mode was in most cases set to $2 \cdot 10^{-9}$ m. The number density of nucleated particles was estimated from the change of total particle number density during the nucleation event.

Determination of particle growth rates from experimental data have previously been carried out by McMurry and Wilson (1982), and Juozaitis et al. (1996) with the goal of extracting "growth laws" from successive size distribution measurements. Our simulations, however, represent another way of studying the process. Whereas the goal of the McMurry-Wilson technique is to extract the growth mechanism from the measured size distributions, we take a reversed approach (although one that relies on size distributions measured at a single location, just like the growth law-technique). We assume a growth mechanism, and try to determine whether or not the best simulation curve fits the measurement data. Because of the different growth laws associated with different growth mechanisms (condensation, surface reaction, volume reaction), it is apparent that the shapes of growth curves resulting from the three mechanisms are different. Therefore, success in reproducing the measured growth curve indicates that the assumed growth mechanism is correct. Fig. 6 illustrates what we mean by a simulation curve fitting or not fitting the measurement data. The points were read (before any simulations were made) from the leading edge of the "growth band" of 15 April shown in Fig. 3 (Toivonen 1997), and thereby represent the growth of the particles that were the first ones to nucleate on that day. Of the three simulated curves, curves (a) and (b) obviously fit the datapoints well, whereas curve (c) tends to show too rapid growth towards the evening. However, also curve (c) is the "best fit" with the specific assumption that the saturation vapour density of species X is 10^5 cm^{-3} (see below for details). If one tries to make the right end of curve (c) fit the datapoints by adjusting the production term of X, the simulated morning growth will become noticeably slower than the

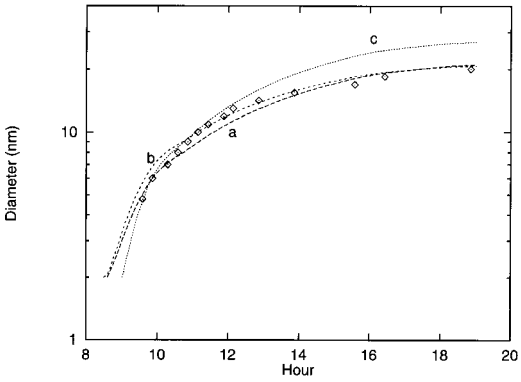

Fig. 6. Growth of nucleation mode particles in 15 April. The diamonds are points read from the leading edge of the observed growth band shown in Fig. 3. Curve (a): the simulation curve shown in Fig. 3. Curve (b): simulation curve with variation of temperature and R.H. as described in subsection 4.2.3. Curve (c): as curve (a), but saturation vapor density of species X is taken to be 10^5 cm^{-3}.

datapoints show. We thus deduce, that the assumption made (in this case regarding the saturation vapour density) leads to a shape of the growth curve that is not in accord with reality, and therefore that specific assumption is most probably incorrect.

During a simulation, we include all the possible parameters from empirical data such as the amount of pre-existing particles, intensity of light, as well as temperature and humidity. Thereby, all the prevailing properties of the system change during the period. This variability results in a slightly winding shape of the simulation curves, and they do not follow the ideal growth laws very smoothly. However, the curves do tend to follow the nucleation mode movements in the experimental data. As explained above, the measured temperatures and relative humidities are not necessarily the same as those experienced by the actual particles during their growth, but as shown below, this will not alter our main result, an order-of-magnitude estimate of the vapour density of the condensing species X.

The simulated growth curves (black curves) of the mean radii of nucleation mode particles during the analysed ten days are shown in Figs. 3, 4. In these simulations, the vapour pressure of X over the surface of the solution droplet was taken to be zero. The molecular weight of X was assumed

to be 100 and diffusion coefficient 0.09 cm^2/s. In these curves the co-condensation of water has been accounted for, as explained above. As can be seen, the curves are in good agreement with the experimental data.

The time-dependent concentrations of the condensing molecules during the simulations are presented in Fig. 7. The daily maximum vapour concentration of the condensing molecules during the simulation varied from about $2 \cdot 10^7\ cm^{-3}$ to $2 \cdot 10^8\ cm^{-3}$. The maximum is typically reached simultaneously with the appearance of the nucleation mode or within 1–2 hours. During most of the days, the maximum is quite flat. However, there are three days with significantly peaked maxima. The vapour concentration is correlated neither with temperature nor with particle number concentration. There is a seasonal trend, however, as the vapour concentrations tend to be higher in the summertime. The growth to rather large sizes during the June events can be explained by the integrated areas of the curves of 8 and 10 June 1996, in Fig. 7.

In order to analyse the sensitivity of the modeled growth curves to different factors, we varied the source term of the condensing molecules, the molecular properties of species X that appear in the condensation equations, and the most important meteorological factors, i.e. temperature and relative humidity.

4.2.1. Sensitivity to source term. In the above calculations the source term of species X was taken to depend on radiation. To study the sensitivity of the results to this assumption, we set the source term constant throughout the growth period. As a result, the growth would be more rapid towards the evening compared with simulations applying a radiation-dependent source term. Thus, the resulting curves are similar to curve (c) in Fig. 6, although with most of the simulated days the deviation from the radiation-dependent curves was not quite as much as the difference between curves (a) and (c) in Fig. 6. However, the concentration of the condensing molecules was not affected too much by the assumption of constant OH, as the levels remained at about half of the maximum value obtained with radiation-dependent source term. In any case, we feel that these model runs support our view that the actual source term of the condensing molecules is radiation dependent, and that the condensable species is produced by photochemical reactions. One could argue that vertical mixing is caused by radiation, which may be the reason for the apparent discrepancy between constant-source term growth curves and observed growth. However, mixing takes places in the morning, and the assumption of constant source term results in too rapid growth towards the evening, which leads us to favor the photochemical explanation.

4.2.2. Sensitivity to molecular properties. To study the effect of the properties of the X molecules on the condensational growth, one of the ten days was picked for closer examination. In Table 1 descriptions and results of different model calculations are presented using the size distribution data of 15 April 1996. During these simulations the concentration of the source term OH was kept constant (although this assumption leads to growth curves that are not completely satisfactory, it is good enough when sensitivity of the condensable vapour concentration to molecular properties is studied.) For simplicity the concentration of OH was set to the value $10^6\ cm^{-3}$ in every simulation described in Table 1. This should not affect the conclusions of the sensitivity analysis. However, one should note that the absolute concentrations of condensing molecules will increase somewhat if the UV-dependence of OH is taken into account.

The sensitivity of the simulated growth curves to the following molecular properties of species X was studied: (1) Molecular mass of the condensing molecule; (2) Water solubility of the condensing molecule; (3) Sticking probability of the condensing molecule on accumulation mode particles (α in Table 1); (4) Nonzero saturation vapour pressure of the condensing molecule.

The molecular mass of the condensing species (which affects the diffusion coefficient) was found to have only a minor effect on the condensation rate. By changing the molecular mass by a factor of 4, the maximum concentration of the condensing vapour changes by a factor of 1.4. The co-condensation of water molecules has a more significant influence on the mass fluxes. Exclusion of water condensation by assuming that species X is completely water insoluble increases the concentration of the model molecules needed to reproduce the observed growth by a factor of four (Table 1). The change of sticking probability on

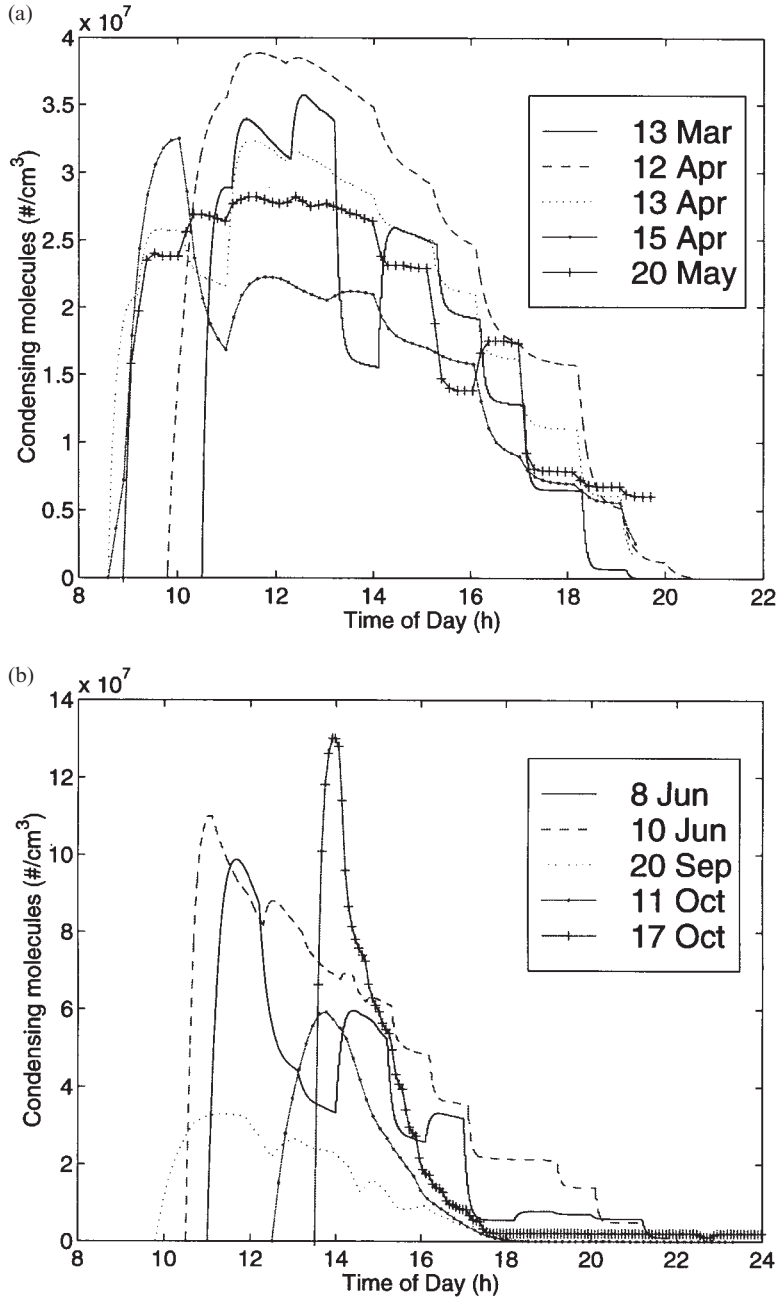

Fig. 7. The gas-phase number density (cm^{-3}) of the condensing species as a function of time on the days shown in Fig. 3, as obtained by the model. Co-condensation of water with species X is included. The stepwise structure of the curve is a result of updating the model with hourly global radiation data. (b) As with (a) but the days correspond to Fig. 4.

Table 1. *Effects of variation of molecular properties and water co-condensation on the precursor and condensing molecule vapor densities*

Water	M	α (acc)	Sat vapour dens	Precursor	Condens mol
y	M	1	0	$1.3 \cdot 10^{10}$	$1.8 \cdot 10^{7}$
y	M	0.001	0	$0.6 \cdot 10^{10}$	$1.6 \cdot 10^{7}$
y	$M \cdot 2$	1	0	$1.3 \cdot 10^{10}$	$2.3 \cdot 10^{7}$
y	$M/2$	1	0	$1.3 \cdot 10^{10}$	$1.4 \cdot 10^{7}$
n	M	1	0	$4.0 \cdot 10^{10}$	$4.7 \cdot 10^{7}$
y	M	1	$1 \cdot 10^{3}$	$1.3 \cdot 10^{10}$	$1.8 \cdot 10^{7}$
n	M	1	$1 \cdot 10^{5}$	$2.1 \cdot 10^{10}$	$2.8 \cdot 10^{7}$
n	M	1	$1 \cdot 10^{3}$	$4.0 \cdot 10^{10}$	$4.7 \cdot 10^{7}$

From left: co-condensation of water allowed (yes/no); molecular mass of condensing molecule ($M = 100$); value of sticking coefficient of condensing molecule on accumulation mode particles; saturation vapour density of condensing species (cm^{-3}); modeled precursor vapour density (cm^{-3}); modeled condensing molecule vapour density (cm^{-3}). In the model calculations, the growth curve was fitted to the data of 15 April 1996 (Figs. 3, 6) as well as possible.

accumulation mode particles does not change the growth properties of nucleation mode significantly. The effect of nonzero saturation vapour density is negligible as long as it remains below 10^3 cm^{-3}. Increasing the saturation vapour density to 10^5 cm^{-3} causes the concentration of condensing molecules to increase by a factor of 1.5. The saturation vapour density cannot be further increased without completely spoiling the agreement between observed growth and modelled growth curve, judging from the slope of curve (c) in Fig. 6. Note that the vapour density discussed here refers to that above the solution surface, not to the saturation vapor density of pure species X.

4.2.3. Sensitivity to T and R.H. As explained above, it is entirely possible that the observed particles have not been formed close to the measurement location, and they may have experienced markedly different temperatures and relative humidities than those applied in the model calculations. We therefore simulated the growth of April 15 by subtracting a constant of 10°C from the recorded temperatures, and added a constant of 20% to the recorded relative humidities applied in the calculations (however, the R.H. was not allowed to go higher than 99%.) These changes did not affect the shape of the modeled growth curve, and the gas-phase concentration of species X was reduced by less than a factor of 2. One could of course suspect that the shape of the growth curve was unaffected because we used constant differences to recorded temperature and relative humidity. We therefore performed another model run, in which the differences to measured T and R.H. were decreased linearly from -10°C and $+20$% in the beginning of the growth to zero in the end of the growth. The resulting curve is shown in Fig. 6 (curve b); there is very little difference to curve (a) in which measured T and R.H. were applied. These results clearly show that we do not have to combine our aerosol dynamics simulations to a mesoscalic transport model in order to gain order-of-magnitude information about the concentrations of the condensing molecules.

4.2.4. Discussion. The model calculations described above give us clues about the chemical nature of the condensing molecules. For example, it seems unlikely that the condensing molecule X is sulphuric acid, although we cannot totally exclude this possibility. The reason is that the concentration of the precursor P needed to produce the required levels of X were generally higher than the observed SO_2 concentrations (which in most cases were actually below the detection level, 0.1 ppb, of our instrument.) Also, the OH concentration is modeled approximately, and probably overestimates the true values. Furthermore, the vapour concentrations of X shown in Fig. 7 are somewhat higher than the maximum sulphuric acid concentrations observed by Weber et al. (1997) in continental air. Presumably, we would see even higher vapour concentrations just before

the new particles are nucleated if we were able to include the nucleation in our model.

One possibility is that the growth is caused by some organic acid(s) having sufficiently low vapour pressure. Also multicomponent condensation of water, sulphuric acid and an organic acid is possible, but only if ammonia participates in the process (H_2SO_4 tends to drive weaker acids out of water solutions if a neutralizing agent is not present.) In any case, the growth seems to be limited by a species with gas-phase concentration above 10^7 and saturation vapour density below 10^5 molecules per cc.

5. Conclusions

Our experimental data from 1996 show about 50 episodes of the appearance and growth of freshly formed nucleation mode particles. The growth to Aitken mode takes always place within a day. In June the particles grew to 60–70 nm in 10 h. During springtime and in the autumn the growth was slower. The nucleation bursts have typically been observed on sunny days (Mäkelä et al., 1997).

Aerosol dynamical model simulations show that the observed growth of new nucleation mode particles can be described by diffusion/kinetically limited condensational growth. The daily maximum vapour concentration of condensing molecules varied between about $2 \cdot 10^7\ cm^{-3}$–$2 \cdot 10^8\ cm^{-3}$, when temperature, relative humidity and source term OH of the model were taken or estimated from measurement data. Most of the simulations were performed assuming zero saturation vapour density for the condensable product. With saturation vapour densities below $10^5\ cm^{-3}$ the growth of the mean diameter of nucleation mode particles was almost the same as with zero vapour density. If the saturation vapour density is above that value the modeled condensational growth curve is not able to follow the observed growth.

Sensitivity analysis shows that changing the molecular mass of the condensing species (which affects the diffusion coefficient) does not significantly affect the growth. Furthermore, a low sticking probability on accumulation mode particles does not have significant effect. We cannot exclude the possibility that water vapour does not participate in the growth process. However, this would increase the vapour concentrations of the condensing molecules by a factor of 4 compared with the values given above. We also studied the sensitivity of the model results to temperature and relative humidity. Applying a 10°C lower temperature and 20% higher relative humidity than what was observed at the measurement location resulted to less than a factor of two lower vapour concentrations of the condensing molecules. Furthermore, the growth curves were reproduced well when T and R.H. were varied from the measured values. Our order-of-magnitude results of the condensable vapour concentrations are thus justified even though we did not apply our aerosol dynamic model in a Lagrangian sense.

Although we have been able to infer clues about the nature of the molecule/molecules causing the observed growth, we are not at this point able to identify them. To fulfill this task, more measurements about the gas and aerosol composition during nucleation events are needed. However, based on model calculations, it seems, probable that the maximum concentration of the condensing molecules is on the order of 10^7–$10^9\ cm^{-3}$, while their saturation vapour density is below $10^5\ cm^{-3}$.

6. Acknowledgements

This work was supported by the Academy of Finland (project number 36594). The help of Mr. P. Aalto, Mr. P. Keronen, and Dr. (hc) T. Pohja is gratefully acknowledged.

REFERENCES

Aalto, P., Kulmala, M. and Nilsson, E. D. 1995. Nucleation events on the Värriö environmental measurement station. *J. Aerosol Sci.* **26**, S411–S412.

Agarwal, J. K. and Sem, G. J. 1980. Continuous flow, single-particle-counting condensation nucleus counter. *J. Aerosol Sci.* **11**, 343–357.

Charlson, R. J. and Wigley, T. M. L. 1994. Sulfate aerosol and climatic change. *Scientific American* **23**, 48–57.

DeMore, W. B., Margitan, J. J., Molina, M. J., Watson, R. T., Golden, D. M., Hampson, R. F., Kurylo, M. J., Howard, C. J. and Ravishakara, A. R. 1985. *Chemical kinetics and photochemical data for use in stratospheric*

modeling, evaluation no. 7. JPL Publication No. 85-37, NASA.

Fuchs, N. A. and Sutugin, A. G. 1970. *Highly dispersed aerosols*. Ann Arbor Science Publ. Ann Arbor, Michigan.

Jaecker-Voirol, A. 1988. PhD thesis, Universite Louis Pasteur, Strasbourg, France.

Jokinen, V. and Mäkelä, J. M. 1997. Closed loop arrangement with critical orifice for DMA sheath/excess flow system. *J. Aerosol Sci.* **28**, 643–648.

Juozaitis, A., Trakumas, S., Girgzdiene, R., Girgzdys, A., Sopauskiene, D. and Ulevicius, V. 1996. Investigations of gas-to-particle conversion in the atmosphere. *Atmos. Res.* **41**, 183–201.

Kerminen, V.-M. and Wexler, A. S. 1995. Growth laws for atmospheric aerosol particles: an examination of bimodality of accumulation mode. *Atmos. Environ.* **29**, 3263–3275.

Kesten, J., Reineking, A. and Porstendorfer, J. 1991. Calibration of a TSI Model 3025 Ultrafine Condensation Particle Counter. *Aerosol Sci. Technol.* **15**, 107–111.

Knutson, E. O. and Whitby, K. T. 1975. Aerosol classification by electric mobility: apparatus, theory and applications. *J. Aerosol Sci.* **6**, 443–451.

Kousaka, Y., Okuyama, K. and Adachi, M. 1985. Determination of particle size distribution of ultra-fine aerosols using a differential mobility analyzer. *Aerosol Sci. Technol.* **4**, 209–225.

Kulmala, M. 1990. Simulating the formation of acid aerosols. In *Acidification in Finland* (edited by Kauppi, P., Anttila, P. and Kenttämies, K.), 95–110. Springer, Berlin.

Kulmala, M., Kerminen, V.-M. and Laaksonen, A. 1995. Simulations on the effect of sulphuric acid formation on atmospheric aerosol concentrations. *Atmos. Environ.* **29**, 377–382.

Mattila, T., Kulmala, M. and Vesala, T. 1997. On the condensational growth of a multicomponent droplet. *J. Aerosol Sci.* **28**, 553–564.

McMurry, P. H. and Wilson, J. C. 1982. Growth laws for formation of secondary ambient aerosols: implications for chemical conversion mechanisms. *Atmos. Environ.* **16**, 121–134.

Mertes, S., Schröder, F. and Wiedensohler, A. 1995. The particle detection efficiency curve of the TSI-3010 CPC as a function of temperature difference between saturator and condenser. *Aerosol Sci. Technol.* **23**, 257–261.

Mäkelä, J. M., Aalto, P., Jokinen, V., Nissinen, A., Palmroth, S., Markkanen, T., Seitsonen, K., Lihavainen, H. and Kulmala, M. 1997. Observations of ultrafine aerosol particle formation and growth in boreal forest. *Geophys. Res. Lett.* **24**, 1219–1222.

Pirjola, L. and Kulmala, M. 1998. Modelling the formation of H_2SO_4–H_2O particles in rural, urban and marine conditions. *Atmos. Res.* **46**, 321–347.

Reid, R. C., Prausnitz, J. M. and Poling, B. E. 1987. *The Properties of gases and liquids*, 4th edition. McGraw-Hill, New York.

Reischl, G. P. 1991. Measurement of ambient aerosols by the differential mobility analyzer method: concepts and realization criteria for the size range between 2 and 500 nm. *Aerosol Sci. Technol.* **14**, 5–24.

Rudolf, R., Majerowicz, A., Kulmala, M., Vesala T., Viisanen, Y. and Wagner, P. E. 1991. Kinetics of particle growth in supersaturated binary vapor mixtures. *J. Aerosol Sci.* **22**, S51–S54.

Rudolf, R. 1994. *Experimental investigation on condensation of supersaturated acid–water vapor mixtures by means of laser light scattering in a newly developed expansion chamber*. PhD thesis, Department of Experimental Physics, University of Vienna, Austria.

SMEAR Homepage, Internet, "http://honeybee.helsinki.fi/HYYTIALA/smear".

Stolzenburg, M. R. and McMurry, P. H. 1991. An ultrafine aerosol condensation nucleus counter. *Aerosol Sci. Technol.* **14**, 48–65.

Toivonen, A. 1997. *A study of the growth of nucleation mode particles observed at the Hyytiälä forestry station.* MSc thesis (in Finnish). Department of Physics, University of Helsinki, Finland.

Vesala, T., Kulmala, M., Rudolf, R., Vrtala, A. and Wagner, P. E. 1997. Models for condensational growth of binary aerosol particles. *J. Aerosol Sci.* **28**, 565–598.

Weber, R. J., McMurry, P. H., Eisele, F. L. and Tanner, D. J. 1995. Measurement of expected nucleation precursor species and 3–500-nm diameter particles at Mauna Loa Observatory, Hawaii. *J. Atmos. Sci.* **52**, 2242–2256.

Weber, R. J., Marti, J. J., McMurry, P. H., Eisele, F. L., Tanner, D. J. and Jefferson, A. 1997. Measurements of new particle formation and ultrafine growth rates at a clean continental site. *J. Geophys. Res.* **102**, 4375–4385.

Wiedensohler, A., Covert, D. S., Swietlicki, E., Aalto, P., Heinzenberg, J. and Leck, C. 1996. Occurence of an ultrafine particle mode less than 20 nm in diameter in the marine boundary layer during Arctic summer and autumn. *Tellus* **48B**, 213–222.

Winklmayr, W., Reischl, G. P., Lindner, A. O. and Berner, A. 1991. A new electromobility spectrometer for the measurement of aerosol size distributions in the size range from 1 to 1000 nm. *J. Aerosol Sci.* **22**, 289–296.